Journal of Food Engineering 166 (2015) 291–301

Contents lists available at ScienceDirect

Journal of Food Engineering

journal homepage: www.elsevier.com/locate/jfoodeng

A multimodal machine vision system for quality inspection of onions

Weilin Wang, Changying Li *

University of Georgia, College of Engineering, 200 D.W. Brooks Dr., Athens, GA 30602, USA

ARTICLE INFO

Article history:
Received 29 January 2015
Received in revised form 29 April 2015
Accepted 18 June 2015
Available online 18 June 2015

Keywords:
Data fusion
Postharvest
Imaging
RGB-D
X-ray
Hyperspectral
Sensor

ABSTRACT

A multimodal machine vision system was developed to evaluate quality factors of onions holistically and nondestructively. The system integrated hyperspectral, 3D, and X-ray imaging sensors. A LabVIEW program was developed to acquire color images, spectral images, depth images, X-ray images of onions, and measure the weight of onions. With the multimodal data collected, algorithms were developed to calculate the maximum diameter, volume, density, and detect latent defects of onions. Three groups of sweet onions (regular, inoculated with *Burkholderia cepacia*, and inoculated with *Pseudomonas viridiflava*) were tested. Results showed that the system accurately measured the weight (RMSE = 3.6 g), diameter (RMSE = 1.7 mm), volume (RMSE = 16.5 cm^3), and density (RMSE = 0.03 g/cm^3) of onions, and correctly classified 88.9% healthy and defective onions. This work demonstrated a promising approach to evaluate both external and internal quality parameters of onions, which is applicable to onion packinghouses. The proposed system and methods are also potentially applicable to quality inspection of other agricultural products.

1. Introduction

The standards for onion grades in the United States (U.S. Department of Agriculture, 1995) enforce a comprehensive regulation on the quality of commercial onions (*Allium cepa* L.). All fresh onions sold in the U.S. fresh market have to meet certain requirements, such as: diameter greater than 1.5 in., mature, no soft or spongy spot, free from decay/scallians/wet sunscald, free from serious damage or defects, to name a few. In addition to complying laws and regulations, U.S. onion growers tend to maintain a stringent quality inspection standard since a large portion of their produces are stored in cold rooms and controlled atmosphere rooms for a fairly long period (1–6 months). Pathogens in defective onions brought into the storage room can be devastating and sometimes could ruin an entire room of healthy onions. Diseased onions not only cause significant economic losses, but also can affect consumers' health and damage the brand owners' reputation.

In a typical U.S. onion packing house, onions are cleaned in automated sorting lines and then delivered to inspection stations by conveyor belts to be checked by trained inspectors. The labor-intensive human visual inspection (HVI) method, however, has many limitations and drawbacks. First, human are prone to making subjective and inconsistent decisions due to fatigue and distractions. Second, labor shortage in many U.S. onion production states and the rising labor cost inevitably increases the onion post-processing cost while decreases the accuracy of quality inspection. Particularly, onions are susceptible to many postharvest diseases such as sour skin (*Burkholderia cepacia*) and neck rot (*Botrytis allii*) (Schwartz and Mohan, 2008). Disease infections can occur in outer scales first and symptoms on onion surface could be latent in early stages (Mark et al., 2002). Since onions are a multilayered vegetable with thick outer skins, it is difficult to evaluate the internal condition of onions by HVI. In summary, it is highly necessary to develop an automated nondestructive approach to inspect and sort onions effectively and efficiently based on both external and internal traits.

Considerable nondestructive machine vision and sensing techniques have been reported for the quality inspection of agricultural and food products, such as color and grayscale imaging methods (Blasco et al., 2009), VIS/NIR spectroscopy (Nicolaï et al., 2007), spectral imaging (Lu, 2008; Qin et al., 2013), magnetic resonance imaging (Marcone et al., 2013), and electronic nose (Li and Heinemann, 2007). In addition, X-ray imaging has been increasingly investigated as an online inspection tool for internal quality assessment of food and agricultural products (Haff and Toyofuku, 2008; Mathanker et al., 2013). Particularly, line scan X-ray imaging has been proven to be a promising non-contact inspection technique to detect internal defects of several agricultural products such as apples (Mendoza et al., 2010; Shahin et al., 1999). Tollner et al. (2005) demonstrated that X-ray imaging is a promising

* Corresponding author at: College of Engineering, 712F Boyd Graduate Studies Research Center, University of Georgia, Athens, GA 30602, USA.
E-mail address: cyli@uga.edu (C. Li).

http://dx.doi.org/10.1016/j.jfoodeng.2015.06.027
0260-8774/

method to detect defects in sweet onions, such as voids and foreign inclusions.

Many of these techniques have potentials for online quality inspection of onions, and a series of studies have been conducted to develop nondestructive sensing methods to evaluate various quality factors of onions in the past six years. Li et al. (2009) applied gas sensor array and support vector machine to detect sour skin in onion storage room. A multispectral imaging approach (Ruiz-Altisent et al., 2010; Wang et al., 2012a,c) was proposed to distinguish sour skin-infected onions from healthy onions using images at two selected near-infrared wavelengths. Wang et al. (2013) used hyperspectral imaging in 400–1000 nm to quantitatively predict the soluble solids content and dry matter content of onions. Wang and Li (2014) proposed a RGB-D method to measure the size traits of onions based on their point cloud images. Each of these studies evaluated certain quality traits of onions. The quality of an onion bulb, however, is determined by a combination of all important quality factors including size, shape, and defect level. Therefore, to meet the classification demand of onion postharvest handling, a comprehensive and automated evaluation of onion quality is needed.

Multisensor data fusion exploits the synergy in information acquired from multiple sources to make better decisions than using any of the information sources individually (Hall and Llinas, 1997). This technique has gained increasing attentions in nondestructive quality evaluation for fruits and vegetables. Steinmetz et al. (1999) discussed the general strategies for applying multiple sensors to assess the quality of fruits using different levels of data fusion process models. Henningsson et al. (2006) proposed a multiple sensor system to monitor the turbidity of milk with an integration of conductivity meter, density meter, and an optical instrument. Bulanon et al. (2009) applied image registration technique to combine color and thermal images of canopy of orange trees to detect oranges in an orchard. Fricke and Wachendorf (2013) combined the height measured by an ultrasonic instrument with the vegetation indices measured by spectral devices to assess the biomass of legume-grass swards. In many other reported applications (Li et al., 2007; Mendoza et al., 2012; Olafsdottir et al., 2004; Ruiz-Altisent et al., 2006), data fusion techniques were also applied to integrate manually operated measurements together with partially automatic nondestructive measurements.

This work was aimed to design and implement a multimodal system and develop multisensor data fusion algorithms to inspect key external and internal quality properties of onions. The main goal was to investigate a potential online approach to evaluate the quality of onions nondestructively and holistically. Specific objectives of the study were to: (1) select appropriate nondestructive sensing technologies for onion quality inspection and integrate a multimodal machine vision system; (2) design a software program for data acquisition; (3) develop algorithms to measure key onion quality parameters based on the collected multimodal data; and (4) evaluate the performance of the proposed system by a laboratory validation test.

2. Multimodal inspection system

2.1. System design

Aimed at providing a potential online sorting solution, various nondestructive sensing techniques were considered and evaluated in the course of the system design. The sensing capability, cost, and scanning speed of techniques were key factors considered in the system design. The proposed design (Fig. 1) consisted of several machine vision techniques with complementary sensing capabilities: color imaging, RGB-depth (RGB-D) imaging, spectral imaging, and X-ray imaging. The rationales for selecting these image techniques were: color imaging provides spatial and color information of onions; spectral imaging can be used to examine surface blemish and rot of onions; RGB-D sensor can measure size and geometry information of onions based on the topological data it collects; X-ray imaging can be used to detect internal defects and disease infections in onions. The potential of selected technologies on onion quality evaluation have been proven by previous studies (Tollner et al., 2005; Wang and Li, 2014; Wang et al., 2012a). This work focused on the integration of these techniques to make a comprehensive evaluation of the quality of onions.

In the proposed design, an onion sample moves from left to right and is scanned at three sequential stages (Fig. 1(B)). First, onion passes the color camera and RGB-D sensor to acquire color and depth images. Second, a liquid crystal tunable filter (LCTF)-based NIR hyperspectral imager was employed to acquire spectral images of the onion. At last, the sample is scanned by an X-ray line-scanner. For all stages, the onion sample is held by a

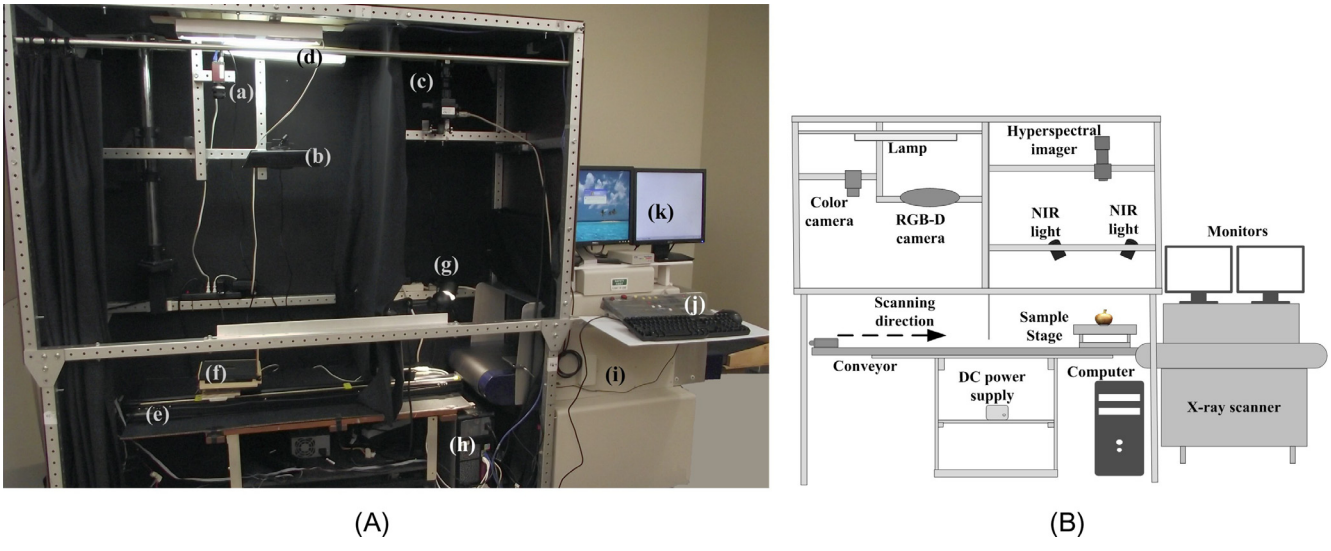

Fig. 1. (A) Components and layout of the system: (a) color camera, (b) RGB-depth sensor, (c) hyperspectral imager, (d) fluorescent lamps, (e) motorized linear slider, (f) onion holder, (g) halogen lamps, (h) computer, (i) X-ray scanner, (j) keyboards, and (k) monitors. (B) Schematic of the multimodal machine vision system for onion quality inspection.

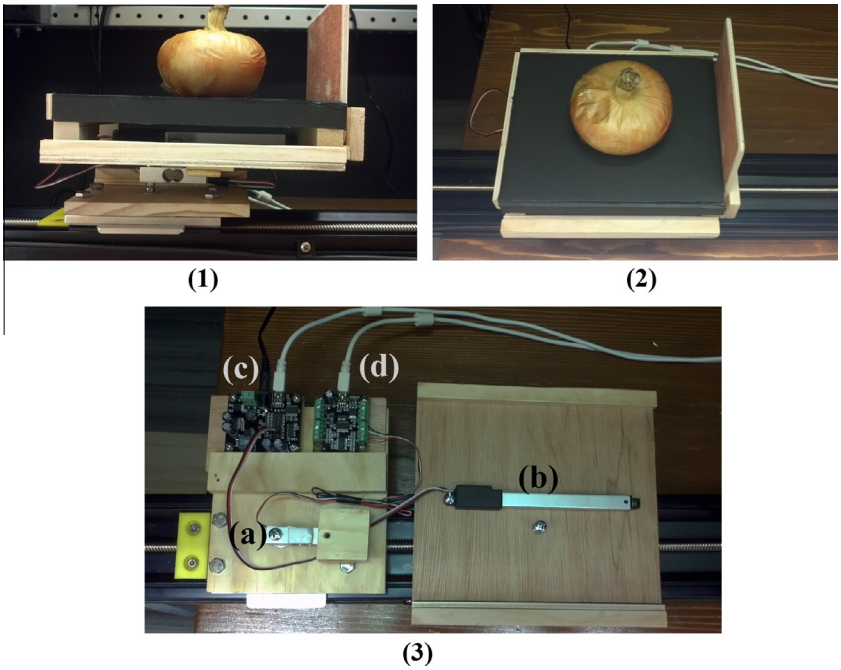

Fig. 2. Illustration of onion scanning stage: (1) side view; (2) top view; (3) sensors used in the stage (the stage was disassembled), including micro load cell (a), linear actuator (b), DC motor controller for linear actuator (c), and Phidget Bridge controller (d).

custom sample holder. A custom weighing device was also added in the onion stage to measure the weight of the sample.

2.2. Multimodal machine vision system

The implemented multimodal machine vision system (Fig. 1(A)) is enclosed in a chamber made from perforated square aluminum tubes and coated wooden panels. A GigE Vision camera (Manta 504c, Allied Vision Technologies, Stadtroda, Germany) was employed to acquire color images (1400 × 1200 pixels) at a speed of 12 frames per second (fps). The camera was connected with the computer by a 2 m long CAT 6 Ethernet cable. RGB-depth sensor (Kinect Sensor, Microsoft, Seattle, WA, USA) was used to acquire depth images of 640 × 480 pixels at the speed of 30 fps and was connected to the computer by a USB cable. The LCTF-based NIR spectral imager (900–1700 nm) consisted of three key components: a 320 × 256 pixels InGaAs camera (SU320KTS-1.7RT, Sensors Unlimited, Inc, Princeton, NJ, USA), a NIR lens of 50 mm focal length (SOLO 50, Sensors Unlimited, Inc., Princeton, NJ, USA), and an LCTF (Varispec LNIR-20-HC-20, Cambridge Research & Instrumentation, Cambridge, MA, USA). For each camera, a custom mounting bracket was made to install the camera on the main frame. The X-ray line-scanner (Model 4262, Autoclear, Fairfield, NJ, USA) has a single X-ray generator operating at 140 kV. The scanner has a 46 × 57 × 27 cm ($W \times L \times H$) scanning tunnel and its conveyor belt (33 cm wide) moves 24 cm per second during scanning. Black curtains were installed inside to separate the two light chambers. In the left chamber, two 18 in. cool-white fluorescent lamps (15 W, 4200 K) with built-in plastic diffuser provided illumination for the color camera. In the second chamber, two 12 V DC halogen lamps (20 W) with glass diffusers were used to provide illumination for the NIR hyperspectral camera.

The multi-layer onion scanning stage (Fig. 2(1)) was mounted on the linear slider motorized by a NEMA 23 motor (MDrivePlus 23, Schneider Electric, CT, USA). The bottom layer of the scanning stage is the mounting base and the customized weighing device (Fig. 2(3)a). The weighing device was made of a micro shear load cell (Model 3133, Phidgets Inc., Alberta, Canada), which can measure weight up to 5 kg with an accuracy of ±2.5 g. The top layer contained an onion holder that consisted of a wooden frame and the top panel (Fig. 2(2)). The top panel was made of 3 mm thick black card board to provide a high contrast and uniform background for images. In addition, the paper panel introduces very little background noise to X-ray images. In the middle layer, a motorized linear actuator (Model L12-100-100-6-R, Firgelli, Victoria BC, Canada) was mounted, which was used as a robotic arm to push the onion holder from the linear slider to the conveyor belt of the X-ray scanner (Fig. 2(3)b).

After system integration, all cameras were aligned and calibrated. The LCTF spectral imaging unit of the system was calibrated following the method introduced in Wang et al. (2012b). The color camera was calibrated using a checker board pattern printed on a letter size paper and a mini color checker card (Munsell mini ColorChecker, X-Rite, MI, USA). The custom weight sensor made from the micro load cell was validated using a 14-piece brass slotted weight set (Carolina Bio. Supply, Burlington, NC, USA).

2.3. Program

A software program was developed to control the scanning process and collect images. The program controls the motorized linear slider to convey the onion to each desired position, and acquires images from each camera. The program also measures the weight information of each onion from the load cell integrated in the scanning stage. The program was written using LabVIEW graphical programming language (2012 sp1, National Instruments, TX, USA). Fig. 3 illustrates the main GUI of the program.

The program consists of multiple modules organized in a state machine model. The module for color images was developed using LabVIEW NI-DAQmx toolbox (National Instruments, TX, USA). The module for acquiring RGB-depth images was developed based on an open source LabVIEW wrapper (https://decibel.ni.com/content/docs/DOC-16978/) for an open source SDK for Kinect sensor (OpenNI, http://www.openni.org/). The modules developed for acquiring hyperspectral images are described in another article

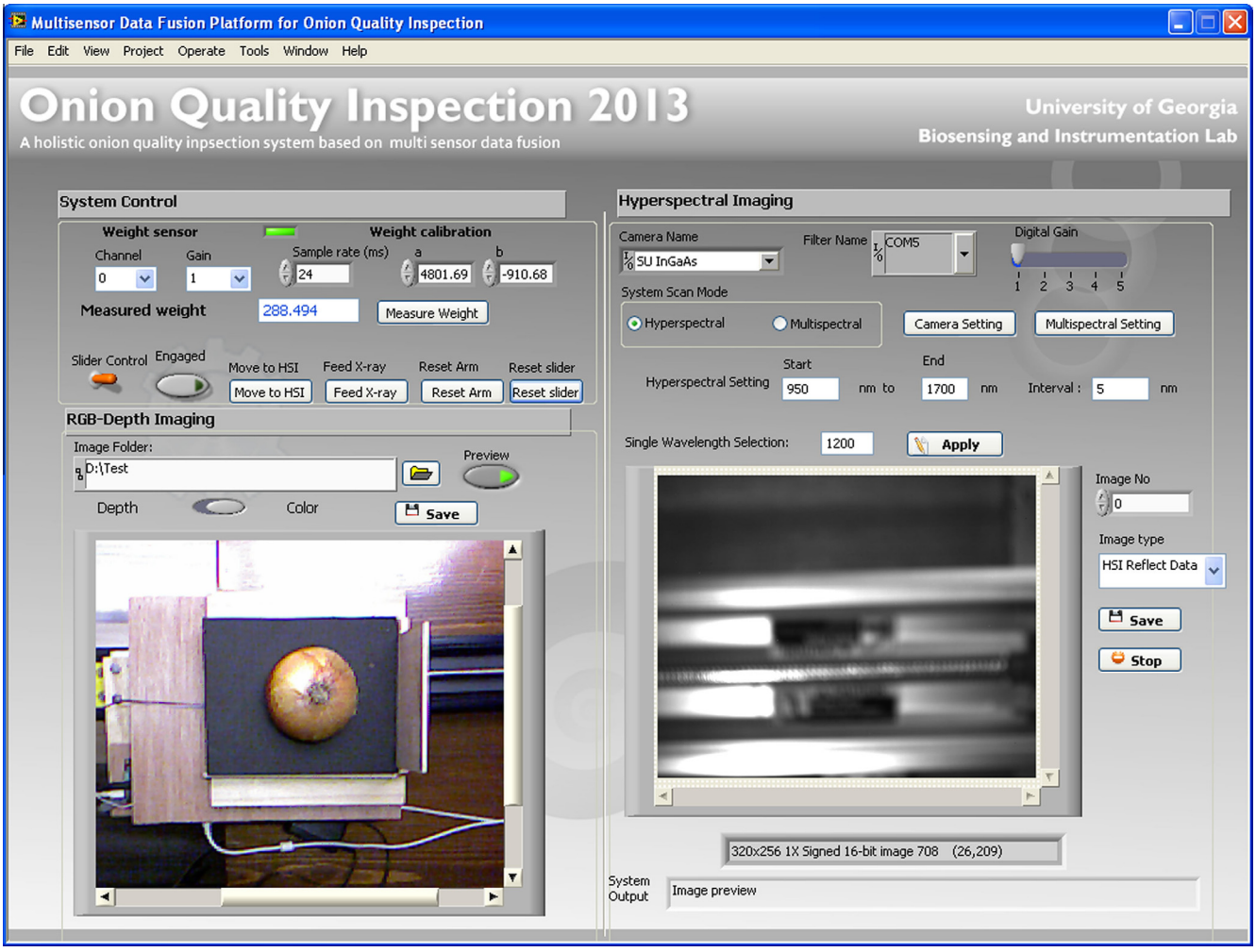

Fig. 3. Main graphic user interface of the onion quality inspection system.

(Wang et al., 2012b) of a previous work. X-ray images were collected by the integrated software program provided by the manufacturer (Autoclear, Fairfield, NJ, USA). The module for weight measurement was developed using the drivers and LabVIEW application program interfaces provided by Phidgets Inc. The module for controlling the motorized linear slider was developed based on the drivers and LabVIEW sub-VIs provided by Schneider Electric Inc.

3. Materials and methods

3.1. Sample preparation

A validation study was conducted to evaluate a number of key onion quality traits: diameter, weight, volume, density, and defect situation (with and without disease) using the proposed multimodal onion quality inspection system. Flat-globe shape sweet onions (Granex type) were purchased from local supermarkets in Athens, Georgia, USA. Onions were manually inspected to select bulbs from medium to colossal size without observable surface blemish or defects. The 80 selected onions were first divided into three groups. The first group contained 40 onions without any treatment. The other two groups (20 onions in each) were inoculated with two pathogens: *B. cepacia* (*B. cepacia*) for sour skin (to develop rottenness in outer onion scales), and *Pseudomonas viridiflava* (*P. viridiflava*) for bacterial streak and rot (to develop decay in more internal onion scales). During the inoculation, a suspension of *B. cepacia* and *P. viridiflava* were prepared by mixing pathogens with sterile tap water. Pathogen suspensions (1.5–2 ml per onion) were infiltrated into onions from the root cap area using a syringe with needle. For the *B. cepacia* suspension, the needle was pricked into the second or third scales of onion bulb with a 30–45° angle to the onion root cap. For the *P. viridiflava* suspension, the needle was stabbed into the onion bulb perpendicular to the onion root cap so that the bacterial suspension was injected into the 4th or 5th scale or deeper. In summary, there were 80 onions tested in this experiment: (1) 40 regular onions (as controls), which were stored in a refrigerator (5 ± 1 °C) for 2–3 weeks before test; (2) 20 onions inoculated with *B. cepacia*, as samples with sour skin; and (3) 20 onions inoculated with *P. viridiflava*, as samples with bacterial streak and rot. Onions inoculated with *B. cepacia* were placed in an incubator (30 ± 1 °C) for 5–6 days and samples inoculated with *P. viridiflava* were incubated at 28 ± 1 °C for 5–6 days before test. All onions were stored individually in zip lock bags labeled by consecutive integer numbers.

3.2. Experimental procedure

The geometrical and physical parameters (diameter, weight, and volume) of onion samples were manually measured to collect the ground truth. Before being scanned by the machine vision system, the maximum equatorial diameter of each onion was measured by a digital caliper for three times and the average value

was used. The weight was measured by a precision digital scale (±0.01 g) for three times and averaged. After being scanned by the system, the volume of each onion bulb was measured using the water displacement (WD) method. All measurements were conducted at room temperature (20 ± 1 °C).

During scanning, the onion was manually placed on the center area of the holder. The weight of the onion was measured by a custom weighing device, and the result was displayed on the GUI of the system and recorded in a text log file. The scanning stage started under the color camera (the initial position) to acquire color images. Then, the scanning stage moved to the preset positions to take RGB-D and then hyperspectral images (950–1700 nm with spectral intervals of 5 nm), respectively. After being scanned by the hyperspectral imager, the onion holder was pushed onto the conveyor belt of the X-ray scanner by the micro robotic arm embedded inside the scanning stage to take X-ray images. In the meanwhile, the scanning stage returned to the initial position under the color camera. In each scan, one color image, one RGB-D image, one hyperspectral image, and one X-ray image of the onion were collected. Since onions used in this test are flat-globe shape, they were scanned twice at two orientations (neck facing up and root facing up).

After scanning, the onion was first cut open horizontally from the equatorial area and then from neck to root direction, resulting in four separate pieces. The disease and defect situation of the onion was manually evaluated. Based on the inspection, 9 onions (out of 40) in the regular onion group had internal defects at different levels. For onions inoculated with *P. viridiflava*, 18 out of 20 developed observable bacterial streak and rot symptoms and two samples remained to be healthy. All 20 onions inoculated with *B. cepacia* developed different levels of sour skin. It was observed that onions with bacterial streak and rot had more internal decay than onions with sour skin, while surface rottenness of sour skin infected onions was more intensive than onions with bacterial streak and rot.

3.3. Data processing and feature extraction

The maximum diameter and volume of onion were estimated using the depth image collected by the RGB-D sensor. Onion depth images were converted into point cloud images and rotated in 3-D space (X–Y–Z) to make maximum projection on X–Y plane to calculate the maximum diameter of the onion. Onion point cloud image was later converted into vortex image to estimate the volume of the onion using linear regression model. Based on the measured weight and volume, the density of onion was calculated. The detailed algorithms for calculating these traits were described in Wang and Li (2014). The estimated diameter, volume, weight, and density of onions were compared to their corresponding ground truth values. Root mean squared error (RMSE) between the estimated values and the ground truth were calculated to verify the accuracy of the proposed methods.

Hyperspectral images of onions were first converted into percentage image by applying flat field correction. The white reference was collected with a Spectralon reflectance panel and the dark image was collected when the optical entrance of the spectral imager was covered by a black cap. Then, images at the wavelengths 1070 nm and 1400 nm of onion hyperspectral image onions were extracted and converted into log-ratio images $\left(\log_{10}\left(\frac{I_{1070\ \mathrm{nm}}}{I_{1400\ \mathrm{nm}}}\right)\right)$, following the approach introduced by Wang et al. (2012a). The generated log-ratio image of the onion can reflect the moisture distribution on the onion surface, in which a bright pixel indicates a high moisture percentage. When an onion is affected by a pathogen, onion flesh becomes rot and the fluid extracted from onion cells often changes the moisture distribution on the onion surface, particularly in the root and neck area. Therefore, the intensity value and the texture pattern of the log-ratio image of onion root and neck area could provide a clue to identify onion disease infections. The sub-image of onion neck or root area (100×100 pixels or 120×120 pixels, depending on the size of the onion image) was segmented from the log-ratio images. The maximum, mean, and minimum intensity values of the segmented image were calculated as the statistical features. The gray-level co-occurrence matrix (GLCM) of the image was calculated at 0°, 45°, 90°, and 135° angles. Then, textural features (contrast, correlation, energy, and homogeneity) were calculated at each GLCM angle.

X-ray images were preprocessed at several steps for feature extraction. At the first step, an onion X-ray grayscale image (160×160 pixels) was segmented from the X-ray image of the whole imaged scene (including the onion and the onion holder). In the segmented X-ray image, the frames of the onion holder were removed and the image only contained the area of the onion and the central area of the top panel of the onion holder. Since the top panel of the onion holder was made from lightweight card board of very low density, it was almost invisible to the X-ray scanner. Therefore, the segmented X-ray image mainly contains the information of the scanned onion bulb. The onion X-ray image was then filtered by a 3×3 pixel-wise adaptive Wiener filter to reduce the noise. The 2% linear stretching was applied to increase the contrast of the image (Gonzalez and Woods, 2008). A copy of the preprocessed onion X-ray image was then converted into a binary image using a threshold level of 0.9. The threshold level was selected based on preliminary tests on the X-ray images of onions collected in this study. The binary image was reversed and morphological operations were then applied on the binary onion mask to fill the holes inside the region. All the foreground regions in the binary mask image were identified and the largest region was identified as the mask of the onion. The onion mask was then applied to the preprocessed onion X-ray grayscale image to remove the background information. The boundaries of the square area containing the onion were identified to further extract the onion image from the 160×160 pixels X-ray image. The maximum, mean, and minimum intensity values of the pixels in the onion region were calculated. Similar to those features of spectral images, the contrast, correlation, energy, and homogeneity of the extracted onion X-ray image were calculated based on GLCM matrices measured at 0°, 45°, 90°, and 135° angles. All image features extracted from onion X-ray images were saved into a CSV text file. All image processing and feature extraction operations were conducted using custom programs developed in MATLAB 2012b. The scheme used for data processing described above is illustrated in Fig. 4.

3.4. Feature selection and classification

Image features extracted and selected from X-ray images, spectral images and physical parameters of onions measured by the system were normalized and used together to build classifier to distinguish healthy onions from diseased onions. Out of four measured physical parameters of onions (weight, diameter, volume, and density), only the diameter and density were used in the classification models since the density of an onion is highly correlated with its weight and volume.

Feature reduction and selection is crucial to the success of this application since this multimodal system involved large amount of data at different domains. Only relevant features contributing to classification should be used to reduce the processing time and defy the curse of dimensionality. In this work, variable selections were conducted on the image features. For the X-ray or spectral image dataset, t-tests ($\alpha = 0.05$) were conducted on each feature to check the difference between the mean of defective onions and the mean of healthy onions. Then, features were sorted based

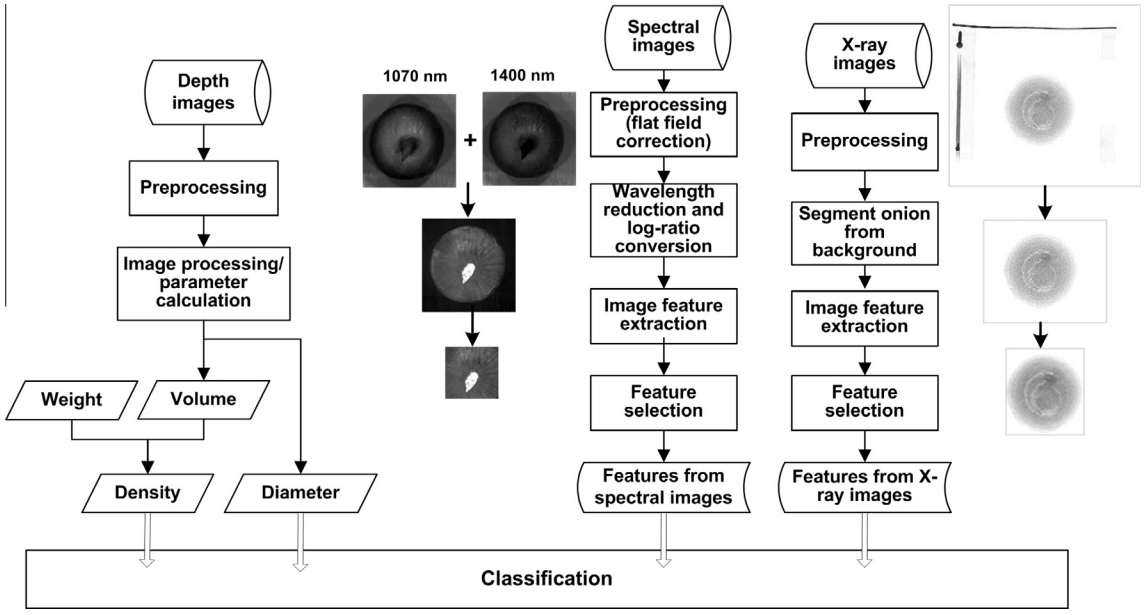

Fig. 4. Flowchart of data processing and feature selections of multimodal image data for onion quality inspection and classification.

on the significance in an ascending order in terms of *p*-value. The dataset of extracted image features were divided into a training dataset (2/3) and a testing dataset (1/3). Support vector machine (SVM) classifiers were developed using the training dataset with incrementally increased numbers of features, and validated using the testing dataset. Classification errors (%) of the SVM models were calculated to check the effect of including more features in the classifier. The optimal number of features was determined when the error of the classifier reached the minimum and later increased when additional features were included.

After feature selection, a number of classifiers were developed and tested in this work using different schemes (Fig. 5). SVM classifiers with radial basis function kernel were trained by the training dataset and then tested using the testing dataset. The optimal parameters (C and gamma) of the tested SVMs were selected by applying the grid search. The first scheme (Fig. 5(a)) tested the classification performance using each individual data source. Image features selected from X-ray images, spectral log-ratio images, and other measured physical parameters were used to construct classifiers, respectively. Optimal features were selected using the method introduced in the previous paragraph.

In the second scheme (Fig. 5(b)), optimal classification models were cascaded and combined to make classification at the decision level. Using this ensemble classifier, the samples passed inspections in the first classifier were further checked by the next classifier. Onions that were suspicious to any classifier were sorted as "diseased". The third classification scheme (Fig. 5(c)) combined all aforementioned selected features and used them to train one single classifier, which is known as the data fusion at the feature level. All feature selections and classification models developed in these schemes were implemented in MATLAB.

4. Results and discussions

4.1. Examples of multimodal images of onions

Fig. 6 illustrates the multimodal images of onions acquired using the proposed machine vision and algorithms, which include color, depth, X-ray, and spectral images of onions. As shown in the figure, disease symptoms of onions with bacterial streak or sour skin were shown in both X-ray and spectral images. On X-ray images, the white areas and short-arc white lines indicate the internal voids and gaps inside the onion. The white (high intensity) spot on onion spectral images reflects the high moisture content area on the surface and outer scales of the onion. Overall, onions with bacterial streak showed more distinguishable textural patterns than those of onions with sour skin on X-ray images, while disease symptoms shown on the spectral log-ratio images of sour skin onions were more obvious than those of bacterial streak onions.

4.2. Results of the measurement of onion physical parameters

The estimated maximum diameters of onions (Fig. 7(a)) well matched (RMSE = 1.7 mm) the reference values manually measured with the caliper. Considering that the onion samples had an average diameter about 100 mm, this accuracy (>98%) was fully adequate for onion production. The onion volume estimated using the depth image (Fig. 7(b)) showed an average error of 15.7 cm^3 compared to the volume measured using water displacement method, resulting in an accuracy of 96.9%, which is comparable to or higher than other reported studies of measuring the volume of fruits and vegetables.

It is shown that the system accurately measured the weight of onions, resulting in an average RMSE of 3.6 g (Fig. 7(c)). This accuracy is lower than what a typical commercial benchtop precision balance provides (in the range of 0.001–0.1 g). The accuracy of the micro load cell used in this test was about ±2.5 g. The accuracy of the weight device can be further enhanced by improving the design of the weighing device. On the other hand, considering the average weight of the tested onion was about 400 g, the relative error of weight measurement using this system was less than one percent, which is adequate for onion grading and packing.

The RMSE of the onion density estimated using the system was 0.029 g/cm^3 (Fig. 7(d)). The reference value was measured by the benchtop precision balance and the volume measured by water displacement. It is known that onion density is related to its dry matter content. Also, the density of an onion could significantly

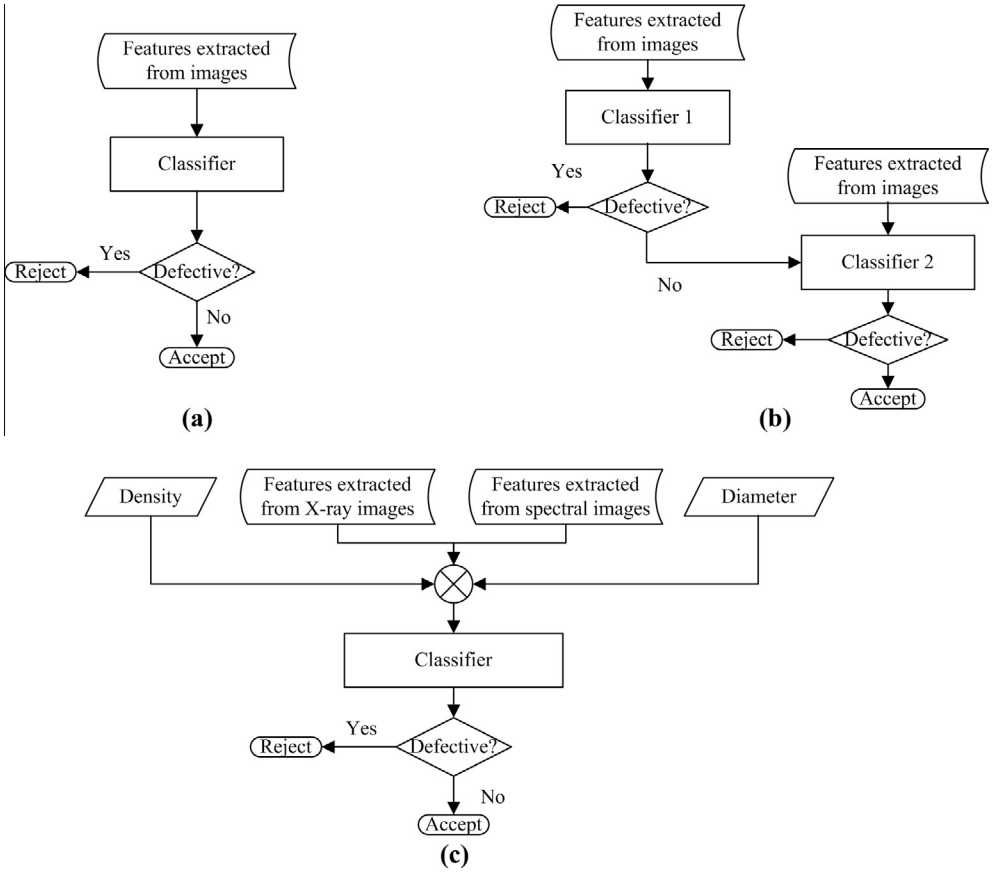

Fig. 5. Classification schemes based on features extracted from multiple data sources: (a) single classifiers using features extracted from each data source, (b) a cascade classifier combined independent classifiers by applying data fusion at the decision level, and (c) a classifier applied data fusion at the feature level.

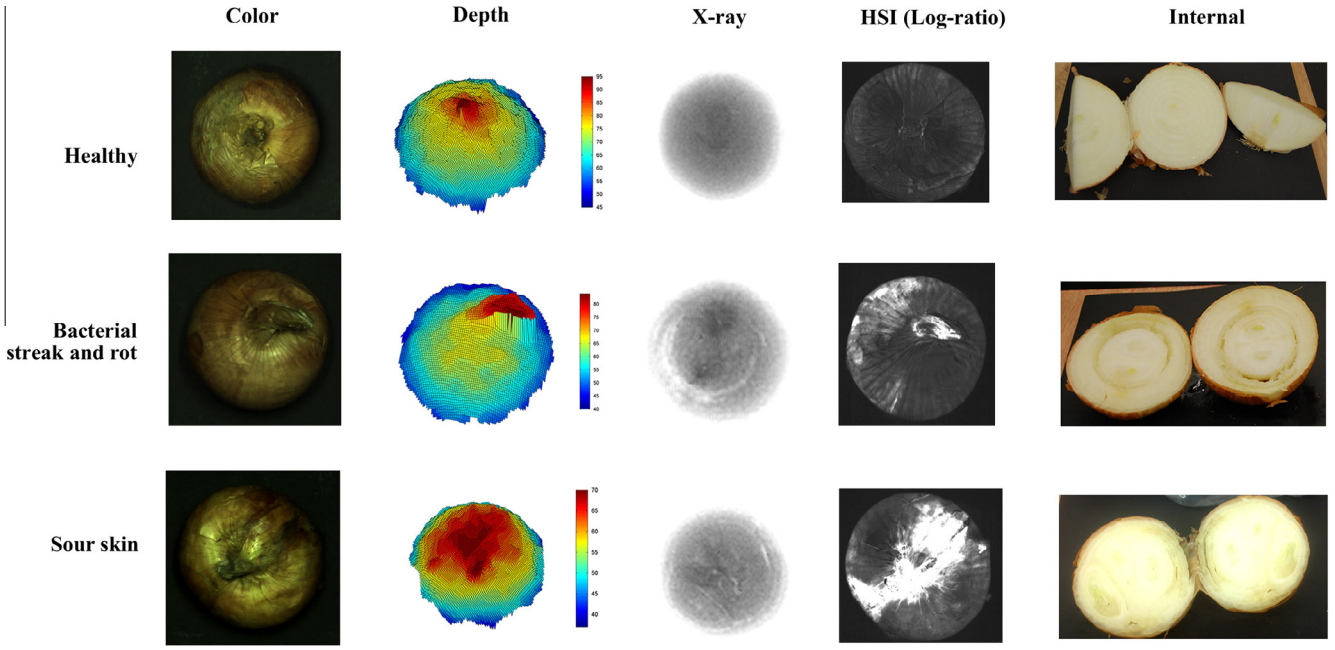

Fig. 6. Examples of preprocessed multimodal images of three onions scanned by the proposed machine vision system. The images at the last column are color pictures of onions cut open after being scanned by the system.

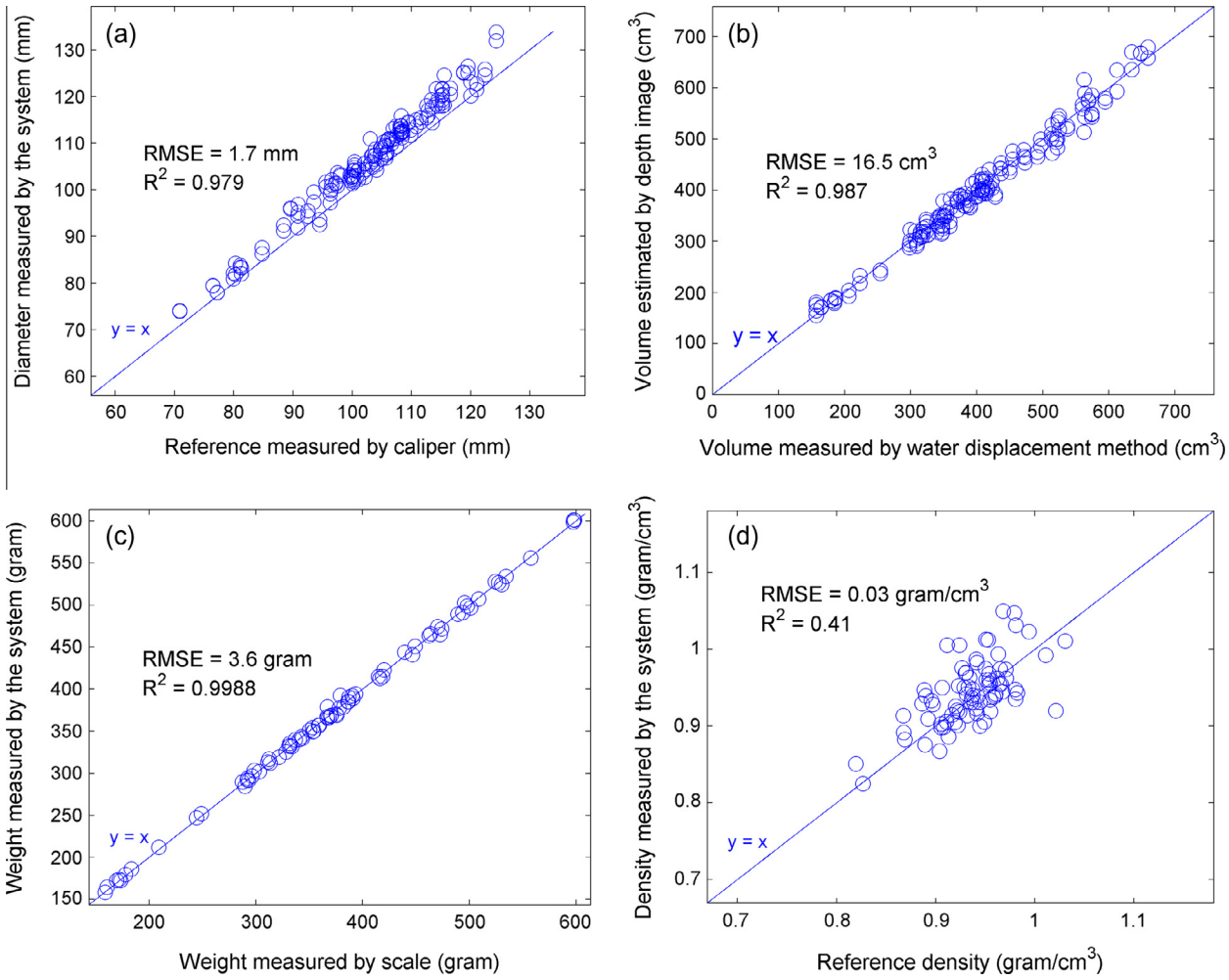

Fig. 7. Results of the four physical parameters of onions measured using the proposed system: (a) diameter, (b) volume, (c) weight, and (d) density.

change when it has disease or defect. Thus, the system's capability to measure density nondestructively provides a potential useful method to evaluate onion quality.

4.3. Results of classification

Feature selections conducted on the X-ray and spectral image datasets improved the classification accuracy (Fig. 8). In the feature selection on X-ray images, the lowest error rate (22.2%) was first achieved by the SVM using four features, which was 1.8% lower than that of using all features (Fig. 8(a)). The four selected image features were the contrast at 45° and 135°, and the homogeneity at 45° and 90°. This is reasonable since the X-ray images of onions with internal defects had contrast and homogeneity values different from those of healthy onions. When internal voids or rottenness occur, the density values of those regions are often significantly reduced, which were shown as bright lines and regions in the X-ray images of onions. As a result, the contrast of onion X-ray images increased and homogeneity decreased. The selected contrast and homogeneity features were mainly at diagonal orientations. This should be caused by the spherical layered structure of onions, which were shown as ring patterns in X-ray images. Thus, those lines, arcs, and areas indicating defective onion area were easier to be detected at diagonal directions.

Ten features were selected from onion log-ratio images, resulting in a lowest error of 27.8% (Fig. 8(b)), which was 5.5% lower than that of using all features. The selected features included four contrast features, four homogeneity features, the mean intensity, the correlation feature at 135°, and the energy feature at 90°. This result generally matched with a previous study (Wang et al., 2012a) for distinguishing sour skin onions from healthy onions: contrast and homogeneity image features contributed the main discrimination power. A main difference was the inclusion of the maximum intensity. In Wang et al. (2012a), the maximum intensity was identified as one of the most indicative log-ratio image features, while in this work the mean intensity was selected instead of the maximum intensity. The main reason for this difference is that the defective samples used in this study included not only sour skin onions but also naturally defective onions and inoculated bacterial steak onions. In spectral log-ratio images of onions, the maximum intensity indicates the highest moisture level on the onion surface. Many of internal defective samples tested in this study did not have distinct surface rot symptoms in their log-ratio images. As a result, the maximum values of log-ratio images of these onions were relatively low. Thus, the maximum intensity was less indicative than the mean intensity in this test.

The SVM with the selected features extracted from onion X-ray images ($SVM_{X\text{-}ray}$) successfully classified 77.8% onions (Table 1). For onions without any inoculation, the classifier missed three defective onions. In the group of onions with bacterial streak and rot, it misclassified one healthy onion and missed a defective one. For onions with sour skin, the performance of $SVM_{X\text{-}ray}$ was quite low (50%). The overall accuracy achieved by the $SVM_{X\text{-}ray}$ is much lower than the classification rates (about 90%) reported by

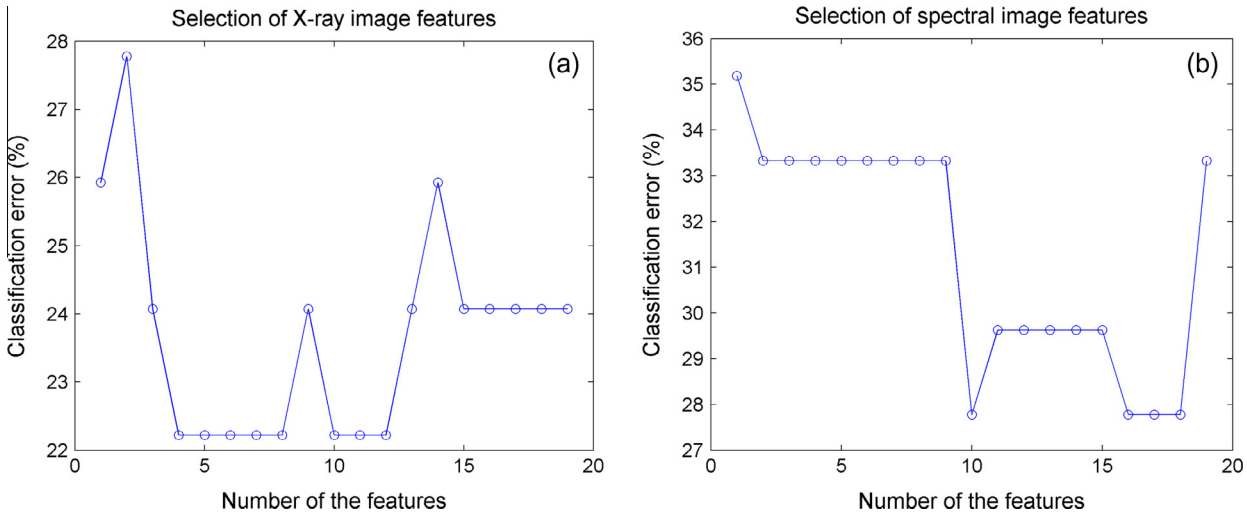

Fig. 8. Feature selections on X-ray image (a) and spectral image (b) data of onions.

Table 1
Classification results of the SVM based on onion X-ray image features, the SVM based on spectral image features, and the SVM classifier using diameter and density.

Classifier	Treatment group	Match		Mismatch		Accuracy (%)	Total accuracy (%)
		Healthy	Defective	False positive	False negative		
SVM using X-ray image features	Regular	21	3	0	3	88.9	
	Bacterial streak and rot	0	11	1	1	84.6	77.8
	Sour skin	0	7	0	7	50.0	
SVM using spectral log-ratio image features	Regular	21	1	0	5	81.5	
	Bacterial streak and rot	1	5	0	7	46.2	72.2
	Sour skin	0	11	0	3	78.6	
SVM using diameter and density	Regular	17	2	4	4	70.4	
	Bacterial streak and rot	1	10	0	2	84.6	63.0
	Sour skin	0	4	0	10	28.6	

Tollner et al. (2005) and Shahin et al. (2002). The main reason for this difference is that this study included a large number of sour skin samples that only had disease symptoms on external layers, while the studies of Tollner et al. (2005) and Shahin et al. (2002) focused on testing onions with internal diseases such as center rot and neck rot.

On the contrary, the classifier using features extracted from spectral images ($SVM_{spectral}$) accomplished a much higher accuracy on the sour skin onion samples, while had a lower performance on the bacterial streak onions. The classification accuracy of $SVM_{spectral}$ on the regular onions was also 7.4% lower than that of $SVM_{X\text{-}ray}$. As confirmed by cutting onions open after scanning, defective onions in the first two groups (regular and bacterial streak) had more internal rot than those in the third group (sour skin), while the sour skin onions developed more intensive surface rot. Thus, results indicate that the $SVM_{X\text{-}ray}$ was more capable to identify onions with internal defects and the $SVM_{spectral}$ performed better in distinguishing onions with surface rot from healthy ones.

The SVM classifier using the measured physical features (diameter and density) of onions ($SVM_{physical}$) had a relatively low accuracy compared to those of $SVM_{X\text{-}ray}$ and $SVM_{spectral}$ (Table 1). However, the classification rate of $SVM_{physical}$ on the bacterial streak group was high (84.6%). This should be mainly attributed to the density of onion. Onions inoculated with bacterial streak had internal decay, which had a lower density than other onions with similar size. Thus, classifier using onion diameter and density features can detect the difference. On the other hand, although the classification accuracy of the $SVM_{physical}$ was identical to that of $SVM_{X\text{-}ray}$, it missed one more diseased onion (false negative) than $SVM_{X\text{-}ray}$. Similar pattern was observed in the group of regular onions. Thus, the $SVM_{physical}$ was less capable than the $SVM_{X\text{-}ray}$ in terms of detecting onions with internal defects. The classification results using sensing data with different features showed that every type of data is useful for the detection of defective onions. X-ray and spectral images of onions could provide complementary clues to evaluate the conditions of onions. The physical parameters measured by the system (diameter and density) also showed evidence of being useful in the recognition of defective onions.

The ensemble SVM with cascaded $SVM_{X\text{-}ray}$, $SVM_{spectral}$, and $SVM_{physical}$ accomplished a total accuracy of 88.9%, which is more than 10% higher than the accuracy of any SVM using single modular data (Table 2). The accuracy of the SVM using features selected from multiple data sources was 3.7% higher than any SVM using single modular data, while 7.4% lower than that of the ensemble SVM. After further feature selection, three optimal features (contrast at 135° of X-ray image, correlation at 135° of spectral image, and homogeneity at 45° of spectral image) were used to build a single classifier, which achieved an accuracy of 5.5% higher, while was still slightly lower than that of the ensemble SVM. This also confirmed that X-ray and spectral image features are strong indicators of onion diseases since neither diameter nor density was not included.

The ensemble SVM employed a stringent voting mechanism at the decision making: labeled an onion as defective if it received a vote from any of those three SVMs. The ensemble SVM only missed one defective onion in the regular group and successfully detected all diseased onions in bacterial streak group and sour skin group. Due to the strict screening criterion, the false positive of the

Table 2
Classification results of the three SVM classifiers developed based on data fusion.

Classifier	Onion treatment	Match		Mismatch		Accuracy (%)	Total accuracy (%)
		Healthy	Defective	False positive	False negative		
Ensemble SVM with three cascaded SVMs	Regular	17	5	4	1	81.5	
	Bacterial streak and rot	0	12	1	0	92.3	88.9
	Sour skin	0	14	0	0	100.0	
Single SVM classifier using all selected X-ray, spectral image, and physical features	Regular	18	4	3	2	81.5	
	Bacterial streak and rot	1	10	0	2	84.6	81.5
	Sour skin	0	11	0	3	78.6	
Single SVM classifier with three optimal X-ray and spectral image features	Regular	20	4	1	2	88.9	
	Bacterial streak and rot	0	10	1	2	76.9	87.0
	Sour skin	0	13	0	1	92.9	

ensemble SVM was also relatively high. On the contrary, the SVM using three optimal X-ray and spectral image features (data fusion at the feature level) showed a higher false negative and a lower false positive. These results generally confirmed that sensor fusion based on X-ray and spectral imaging can achieve higher classification accuracy than using any of these single sensing methods. It has to be noted that these classification accuracies were evaluated based on a lab validation experiment with inoculated onions. The performance of the proposed classifiers on natural onions in packinghouse will be tested in the future study.

Overall, the lab experiment verified the sensing capability of the proposed multimodal machine vision system for onion classification. Using the multimodal sensing data collected with hyperspectral, X-ray, and 3-D depth sensors, a holistic quality assessment algorithm can be studied and applied to make a classification decision that is more comprehensive and accurate than that of using conventional onion sorting systems. With a reasonable cost and effort, these imaging techniques can be adapted and integrated into regular machine vision-based onion sorting system. For instance, multispectral and RGB-D techniques can be included in color camera-based inspection station, and a line-scan X-ray imaging inspection station can be added into the onion sorting pipeline in the packinghouse. Although the scanning speed of this proposed proof-of-concept system is low (one onion per minute), all these imaging techniques can be scaled up in a high throughput manner in real applications. In addition to the onion quality parameters demonstrated in this article, the proposed system has a great potential to evaluate many other quality traits of onions (i.e. dry matter content, sunscald, the uniformity of onion size) that can be employed to make advanced sorting decisions for onions.

5. Conclusions

A novel multimodal machine vision system utilizing spectral, X-ray, and 3-D depth imaging technologies was designed for quality inspection of onions. A LabVIEW program was also developed to control and synchronize hardware devices for data acquisition. The system can nondestructively acquire comprehensive information of onions in color, 3-D, spectral, and X-ray imaging domains. The laboratory test showed that the proposed system accurately measured the diameter (RMSE = 1.7 mm), volume (RMSE = 16.5 cm^3), weight (RMSE = 3.6 g), and density (RMSE = 0.03 g/cm^3) of the tested onions. Classifiers using selected image features of X-ray and spectral images were able to detect onions with either external or internal rot, or both. X-ray imaging and spectral imaging demonstrated a complementary sensing capability in recognizing defective onions. When information collected from multiple sensors were fused at the decision level or at the feature level, the detection rates of defective onions were higher than those classifiers using information extracted from a single image source.

The proposed multimodal system demonstrated an enhanced sensing capability than the conventional classification systems for fruits and vegetables. In the future, the proposed multisensor-based machine vision system can be used to measure additional onion quality properties, and to grade onions using more comprehensive criteria. The presented system and methods can also be potentially extended for postharvest quality inspection of other agricultural products.

Acknowledgements

This work was funded by the USDA NIFA Specialty Crop Research Initiative (Award No. 2009-51181-06010). Authors also sincerely acknowledge Mr. Anthony Mason Dean, Mr. Paul Glatz, Ms. Delmaries Gonzalez, and Ms. Amber Leigh Stewart for their technical assistance in this project.

References

Blasco, J., Cubero, S., Mira, P., Molt, E., 2009. Development of a machine for the automatic sorting of pomegranate (*Punica granatum*) arils based on computer vision. J. Food Eng. 90, 27–34.
Bulanon, D.M., Burks, T.F., Alchanatis, V., 2009. Image fusion of visible and thermal images for fruit detection. Biosyst. Eng. 103, 12–22.
Fricke, T., Wachendorf, M., 2013. Combining ultrasonic sward height and spectral signatures to assess the biomass of legume–grass swards. Comput. Electron. Agric. 99, 236–247.
Gonzalez, R., Woods, R.E., 2008. Digital Image Processing, third ed. Pearson Prentice Hall, Upper Saddle River, New Jersey.
Haff, R.P., Toyofuku, N., 2008. X-ray detection of defects and contaminants in the food industry. Sens. Instrum. Food Qual. Safe. 2, 262–273.
Hall, D.L., Llinas, J., 1997. An introduction to multisensor data fusion. Proc. IEEE 85, 6–23.
Henningsson, M., Östergren, K., Sundberg, R., Dejmek, P., 2006. Sensor fusion as a tool to monitor dynamic dairy processes. J. Food Eng. 76, 154–162.
Li, C., Gitaitis, R., Tollner, B., Sumner, P., MacLean, D., 2009. Onion sour skin detection using a gas sensor array and support vector machine. Sens. Instrum. Food Qual. Safe. 3, 193–202.
Li, C., Heinemann, P., Sherry, R., 2007. Neural network and Bayesian network fusion models to fuse electronic nose and surface acoustic wave sensor data for apple defect detection. Sens. Actuators B: Chem. 125, 301–310.
Li, C., Heinemann, P.H., 2007. ANN-integrated electronic nose and zNose system for apple quality evaluation. Trans. ASABE 50, 2285–2294.
Lu, R., 2008. Quality evaluation of fruit by hyperspectral imaging. In: Da-Wen, S. (Ed.), Computer Vision Technology for Food Quality Evaluation. Academic Press, pp. 319–348.
Marcone, M.F., Wang, S., Albabish, W., Nie, S., Somnarain, D., Hill, A., 2013. Diverse food-based applications of nuclear magnetic resonance (NMR) technology. Food Res. Int. 51, 729–747.
Mark, G.L., Gitaitis, R.D., Lorbeer, J.W., 2002. Bacterial diseases of onion. In: Rabinowitch, H.D., Currah, L. (Eds.), Allium Crop Science: Recent Advances. CABI Pub., Wallingford, Oxfordshire, UK.

Mathanker, S.K., Weckler, P.R., Bowser, T.J., 2013. X-ray applications in food and agriculture: a review. Trans. ASABE 56, 1227–1239.
Mendoza, F., Lu, R., Cen, H., 2012. Comparison and fusion of four nondestructive sensors for predicting apple fruit firmness and soluble solids content. Postharvest Biol. Technol. 73, 89–98.
Mendoza, F., Verboven, P., Ho, Q.T., Kerckhofs, G., Wevers, M., Nicolaï, B., 2010. Multifractal properties of pore-size distribution in apple tissue using X-ray imaging. J. Food Eng. 99, 206–215.
Nicolaï, B.M., Beullens, K., Bobelyn, E., Peirs, A., Saeys, W., Theron, K.I., Lammertyn, J., 2007. Nondestructive measurement of fruit and vegetable quality by means of NIR spectroscopy: a review. Postharvest Biol. Technol. 46, 99–118.
Olafsdottir, G., Nesvadba, P., Di Natale, C., Careche, M., Oehlenschläger, J., Tryggvadóttir, S.A.V., Schubring, R., Kroeger, M., Heia, K., Esaiassen, M., Macagnano, A., Jørgensen, B.M., 2004. Multisensor for fish quality determination. Trends Food Sci. Technol. 15, 86–93.
Qin, J., Chao, K., Kim, M.S., Lu, R., Burks, T.F., 2013. Hyperspectral and multispectral imaging for evaluating food safety and quality. J. Food Eng. 118, 157–171.
Ruiz-Altisent, M., Lleó, L., Riquelme, F., 2006. Instrumental quality assessment of peaches: fusion of optical and mechanical parameters. J. Food Eng. 74, 490–499.
Ruiz-Altisent, M., Ruiz-Garcia, L., Moreda, G.P., Lu, R., Hernandez-Sanchez, N., Correa, E.C., Diezma, B., Nicolaï, B., García-Ramos, J., 2010. Sensors for product characterization and quality of specialty crops—a review. Comput. Electron. Agric. 74, 176–194.
Schwartz, H.F., Mohan, S.K., 2008. Compendium of Onion and Garlic Diseases and Pests, second ed. APS Press, American Phytopathological Society, St. Paul, Minn.
Shahin, M.A., Tollner, E.W., Evans, M.D., Arabnia, H.R., 1999. Watercore features for sorting red delicious apples: a statistical approach. Trans. Am. Soc. Agric. Eng. 42, 1889–1896.
Shahin, M.A., Tollner, E.W., Gitaitis, R.D., Sumner, D.R., Maw, B.W., 2002. Classification of sweet onions based on internal defects using image processing and neural network techniques. Trans. Am. Soc. Agric. Eng. 45, 1613–1618.
Steinmetz, V., Sevila, F., Bellon-Maurel, V., 1999. A methodology for sensor fusion design: application to fruit quality assessment. J. Agric. Eng. Res. 74, 21–31.
Tollner, E.W., Gitaitis, R.D., Seebold, K.W., Maw, B.W., 2005. Experiences with a food product X-ray inspection system for classifying onions. Appl. Eng. Agric. 21, 907–912.
U.S. Department of Agriculture, 1995. United States standards for grades of onions (other than Bermuda-Granex-Grano and Creole type). U.S. Department of Agriculture.
Wang, H., Li, C., Wang, M., 2013. Quantitative determination of onion internal quality using reflectance, interactance, and transmittance modes of hyperspectral imaging. Trans. ASABE 56, 1623–1635.
Wang, W., Li, C., 2014. Size estimation of sweet onions using consumer-grade RGB-depth sensor. J. Food Eng. 142, 153–162.
Wang, W., Li, C., Tollner, E.W., Gitaitis, R.D., Rains, G.C., 2012a. Shortwave infrared hyperspectral imaging for detecting sour skin (*Burkholderia cepacia*)-infected onions. J. Food Eng. 109, 38–48.
Wang, W., Li, C., Tollner, E.W., Rains, G.C., 2012b. Development of software for spectral imaging data acquisition using LabVIEW. Comput. Electron. Agric. 84, 68–75.
Wang, W., Li, C., Tollner, E.W., Rains, G.C., Gitaitis, R.D., 2012c. A liquid crystal tunable filter based shortwave infrared spectral imaging system: calibration and characterization. Comput. Electron. Agric. 80, 135–144.